Reactions of Cl Atoms with Dimethyl Sulfide: A Theoretical Calculation and an Experimental Study with Cavity Ring-Down Spectroscopy†

Shinichi Enami, Yukio Nakano,‡ Satoshi Hashimoto, and Masahiro Kawasaki*

Department of Molecular Engineering and Graduate School of Global Environmental Studies, Kyoto University, Kyoto 615-8510, Japan

Simone Aloisio

California State University, Channel Islands, One University Drive, California, California 93010

Joseph S. Francisco

Department of Chemistry and Earth & Atmospheric Science, Purdue University, West Lafayette, Indiana 47907-1393

Received: January 16, 2004; In Final Form: April 25, 2004

The adduct formation in the reactions of Cl and Br atom with dimethyl sulfide (DMS) is studied theoretically and experimentally. The rate constants of the forward reaction at several temperatures and pressures are determined from the rise and decay time profiles of the adduct, Cl−DMS, using cavity ring-down laser spectroscopy. The high-pressure limit rate constant for the Cl−DMS adduct formation is determined to be k_{1a}(high) = (2.2 ± 0.2) × 10^{-10} cm^3 $molecule^{-1}$ s^{-1}. The rate constant of Cl with DMS at atmospheric pressure is k_1 = (3.6 ± 0.2) × 10^{-10} cm^3 $molecule^{-1}$ s^{-1}. Error bars are 1σ. The Arrhenius plot of the forward reaction has a negative temperature dependence for 278−318 K. The calculated equilibrium constants of the reaction Cl and Br with DMS at 300 K are K_{ClDMS} = 2.8 × 10^{-12} and K_{BrDMS} = 7.7 × 10^{-15} cm^3 $molecule^{-1}$, respectively. The binding energy (D_0) is calculated to be 17.7 kcal mol^{-1} for Cl−DMS, and 14.1 kcal mol^{-1} for Br−DMS. D_0(Br−C) is in fair agreement with the previously reported experimental value, 12 ± 1 kcal mol^{-1}. The results are discussed in comparison with previous experimental reports of the bromine atom adduct, Br−DMS. Atmospheric implications regarding the fate of the X−DMS adducts (X = Cl and Br) in the troposphere are discussed.

1. Introduction

Dimethyl sulfide (DMS), the largest natural source of atmospheric sulfur, is produced by phytoplankton in the oceans and is released into the atmosphere.[1−5] DMS has been considered to be oxidized by the reactions with OH radicals during the daytime[6,7] and with NO_3 radicals at night time[8−10] to give the oxdized compounds that lead to the formations of aerosol and cloud condensation nuclei. The oxidation reactions of DMS may have a substantial impact on cloud formation over the oceans and influences the Earth's radiation balance and climate system.[11] Recent studies have shown that the reactions of DMS with atomic halogens and halogen monoxide radicals may also play an important role in the sulfur cycles more than previously proposed.[12−15] DMS is present in the marine bundary layer as is the case with chlorine atoms. Cl atoms are produced from sea salt aerosols in the marine boundary layer[12] and react with nonmethane hydrocarbons faster than OH radicals.[16] In the present work we have studied the reactions of DMS with chlorine atoms, which proceed via two reaction channels; one is the addition channel to the sulfur atom (1a) that is pressure dependent, and the other is the hydrogen abstraction channel (1b) that is pressure independent

$$Cl + CH_3SCH_3 + M \rightarrow Cl{-}DMS + M \qquad (1a)$$

$$Cl + CH_3SCH_3 \rightarrow HCl + CH_3SCH_2 \qquad (1b)$$

Stickel et al.[17] reported that the branching ratio of reaction 1b approaches unity with decreasing the total pressure. Urbanski et al.[18] reported the kinetics for Cl−DMS with O_2, NO, and NO_2. To study the fate of the Cl−DMS adduct in the atmospheric condition, we used the cavity ring-down spectroscopy (CRDS) that is an absorption spectroscopy technique based on measurement of the decay of a laser pulse confined within a cavity between two highly reflecting mirrors.[19−23] In 1993, Lin and co-workers reported on the first application of CRDS to kinetics studies by combining CRDS with the laser flash photolysis method, which is called time-resolved CRDS in their paper.[24] They generated nonemissive phenyl radicals from the laser flash photolysis of nitorosobenzene, using time-resolved CRDS to measure the reaction rates.[25−30] After their works, this type of systems has been used in some radical kinetic studies.[15,31−37] The high sensitivity of CRDS enables us to keep

† Part of the special issue "Richard Bersohn Memorial Issue".

* To whom corresponding should be addressed. Fax: + 81-75-383-2573. Email: kawasaki@moleng.kyoto-u.ac.jp.

‡ Present addresses: Faculty of Information Sciences, Hiroshima City University, Hiroshima 731-3194, Japan.

10.1021/jp049772y CCC: $27.50
Published on Web 06/08/2004

TABLE 1: Calculated Bond Distances and Binding Energies of the Cl−S and Br−S Bonds in the Cl−S(CH$_3$)$_2$ and Br−S(CH$_3$)$_2$ Adducts

		bond length (Å) and binding energy (kcal mol^{-1})					
		Cl−S			Br−S		
level of theory	basis set	R_{ClS}	D_e	D_0	R_{BrS}	D_e	D_0
B3LYP	6−311++G(2df,2p)	2.63	23.9	23.1	2.80	19.1	18.4
	6−311++G(3df,3pd)	2.62	24.2	23.4	2.80	19.1	18.3
MP2	6−311++G(2df,2p)	2.50	21.9	21.0	2.66	17.9	17.1
MP4	6−311++G(2df,2p)		18.9	18.0		15.0	14.2
QCISD(T)	6−311++G(2df,2p)		18.6	17.7		14.9	14.1

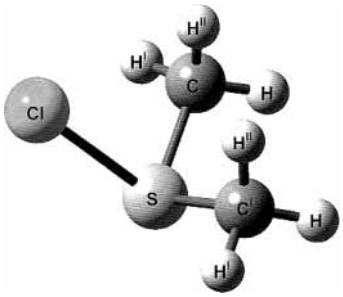

Figure 1. Schematics of the structure of the Cl adduct with dimethyl sulfide.

radical concentrations as low as to reduce the complicated radical−radical reactions.

2. Methods

A. Theoretical Method. The equilibrium geometries of the ground states of the Cl−DMS and Br−DMS adducts were optimized using MP2 and B3LYP methods with the 6-311++G-(2df,2p) basis set, and with the B3LYP method with the 6-311++G(3df,3pd) basis set. Calculations were carried out using the Gaussian 98[38] suite of programs. The spin contamination value, $\langle S^2 \rangle$, before spin projection was 0.7758 for the Cl−DMS and 0.7726 for the Br−DMS. After spin projection, $\langle S^2 \rangle$ was 0.7502 for both Cl−DMS and Br−DMS. There are no significant spin contamination problems associated with the wave function for both Cl−DMS and Br−DMS. The calculated bond lengths are shown in Table 1, and the other structural parameters are listed in supplement Table 1. The structure of Cl−DMS is schematically shown in Figure 1. Br−DMS also has a structure similar to that of Cl−DMS. As listed in Table 1, single-point energies were calculated by using the optimized B3LYP/6-311++G(3df,3pd) geometry using the MP4 and QCISD(T) methods with the 6-311++G(2df,2p) basis set. The vibrational frequencies and rotational constants of the adducts were calculated with the B3LYP method, using the same basis sets as for the optimizations. The results are in Supporting Information Tables 2−5. The basis set used for all higher order electron correlation calculations was the 6-311++g(2df,2p) basis set. To calculate the equilibrium constant, K, for the formation of the X−DMS adducts (X = Cl, Br), the B3LYP/6-311++G(3df,3pd) optimized geometry and calculated frequencies were used. All vibrations were calculated harmonic frequencies. The internal rotations of the methyl groups of the DMS and the adducts were ignored in the partition function calculations. Though this may not be an exact treatment, we feel this is justified because (1) we feel isolated DMS and the adduct will have a similar hindrance to rotation due to the relatively large intermolecular distance between the chlorine atom and the rotating methyl group and (2) the rotation barrier should be similar to that of methanethiol, which is relatively small (1.3 kcal mol^{-1}).

At the QCISD(T) level of theory, the binding energy (D_0) was calculated to be 17.7 kcal mol^{-1} for Cl−DMS and 14.1 kcal mol^{-1} for Br−DMS. The calculated result for Br−DMS is in fair agreement with the experimental value, 12 ± 1 kcal mol^{-1}, reported in our previous paper.[14] There have been three previous computational determinations of the Cl−S bond strength in Cl−DMS: 12.1, 12.3, and 19.3 kcal mol^{-1} depending on the level of theory, QCISD(T)/MP/6-31+G(2d), UQCISD-(T)/DZP/UMP2/DZP, and MP2(Full)/6-311G**, respectively.[39−41] The present calculated value, 17.7 kcal mol^{-1}, is between these values.

Using the following equations along with the results of the theoretical calculations, the equilibrium constants for the formation of the adduct of Cl and Br with DMS were determined:[42]

$$K = \frac{g(\mathrm{XDMS})}{g(\mathrm{X})\, g(\mathrm{DMS})} \frac{\Lambda(\mathrm{X})^3 \Lambda(\mathrm{DMS})^3 V_m}{\Lambda(\mathrm{XDMS})^3 N_A} \times \frac{q^R(\mathrm{XDMS})\, q^V(\mathrm{XDMS})}{q^R(\mathrm{DMS})\, q^V(\mathrm{DMS})} \exp\left(\frac{-D_0}{RT}\right)$$

$$\Lambda = \left(\frac{h^2}{2\pi m k_B T}\right)^{1/2} \qquad q^R = \frac{1}{\sigma}\left(\frac{k_B T}{hc}\right)^{3/2}\left(\frac{\pi}{ABC}\right)^{1/2}$$

$$q^V = \prod_i \left(1 - \exp\left(-\frac{hc\nu_i}{k_B T}\right)\right)^{-1} \qquad (2)$$

where g is the degeneracy of the electronic ground state, V_m is the molar volume, h is the Planck constant, N_A is the Avogadro number, m is the mass of the molecule, k_B is the Boltzmann constant, T is temperature, c is the speed of light, and ν_i is the ith vibrational frequency of a mode. A, B, and C are the rotational constants. A symmetry number (σ) of 1 was used for these calculations, although it may be possible that this species has C_{2v} symmetry due to an out-of-plane (OPLA) vibration with very low barrier.[43] The calculated equilibrium constants of the reaction Cl and Br with DMS are $K_{ClDMS} = 2.8 \times 10^{-12}$ and $K_{BrDMS} = 7.7 \times 10^{-15}$ cm^3 molecule^{-1}, respectively, at 300 K. The calculated equilibrium constant K_{BrDMS} of Br−DMS is in reasonable agreement with that determined experimentally in our previous paper,[14] $K_{BrDMS} = (4.1 \pm 0.3) \times 10^{-15}$ cm^3 molecule^{-1}.

B. Experimental Details. The CRDS apparatus used in the present study has been described in detail elsewhere.[44] Cl atoms were generated by photodisocciation of Cl_2SO at 266 nm (Nd^{3+}: YAG laser; Spectra Physics, GCR-250). The idler output from an optical parametric oscillation laser (Spectra-Physics, MOPO-SL) was frequency doubled with a BBO crystal to obtain the desired probe wavelength. The idler output from the MOPO was frequency doubled with a BBO crystal to obtain the disired wavelength range. The cavity ring-down mirrors (Research Electro Optics, 7.8 mm diameter and 1 m curvarture) had a specified maximum reflectivity of 0.9995 at 350 nm and were mounted 1.04 m apart. Light leaking from the end mirror was detected by a photomultiplier tube (Hamamatsu Photonics, R212UH) with a fast response socket assembly (Hamamatsu Photonics, E5815-01) through a broad band-pass filter (Toshiba, UVD-33S). The active divider makes the linear response range of the photomultiplier tube more than twice that of a conventional divider with a series of resistors. The ring-down signal of the light intensity was sampled by a digitizing oscilloscope (Tektronix, TDS-714L, 500 MHz, 500 MS/s, 8-bit digitizer) and

recorded in a personal computer (PC). The decay of the light intensity is represented by

$$I(t) = I_0 \exp(-t/\tau) = I_0 \exp(-t/\tau_0 - \sigma n c L_R t/L) \quad (3)$$

where I_0 and $I(t)$ are the light intensities at time 0 and t, respectively. τ_0 is the cavity ring-down time without photolysis laser light (about 5 μs at 340 nm), L_R is the length of the reaction region (0.46 m), L is the cavity length (1.04 m), τ is the measured cavity ring-down time with photlysis laser light, and c is the velocity of light. n and σ are the concentration and absorption cross section of the species of interest, respectively. Each ring-down trace was digitized with a time resolution of 20 ns. The digitized traces were transferred to the PC and averaged over 16 or 32 runs to calculate ring-down rate, τ^{-1}. The validity of using the cavity ring-down spectroscopy technique for kinetic studies derives from the fact that the lifetimes of the products generated by photolysis are much longer than the associated cavity ring-down times.[45]

The reaction cell consisted of a Pyrex glass tube (21 mm i.d.), which was evacuated by a combination of an oil rotary pump and a mechanical booster pump. The temperature of the gas flow region was controlled over the range 273−318 K by circulation of a mixture of ethylene glycol and water with a cooling circulator (EYELA, NCB-3100). The difference between the temperature of the sample gas at the entrance and exit of the flow region was <1 K. The pressure in the cell was monitored by an absolute pressure gauge (Baratron, 622A). Gas flows were regulated by mass flow controllers (KOFLOC, 3660). A slow flow of nitrogen diluent gas was introduced at the ends of the ring-down cavity close to the mirrors to minimize deterioration caused by exposure to the reactants and the products. The total flow rate was kept constant at 6.0×10^3 cm^3 min^{-1} (STP). DMS and Cl_2SO were supplied from the glass bulbs, and the concentrations of these gases were calculated by the flow rates of each mass flow controller and reactant concentration in the gas bulbs.

In the study of the Cl + DMS reaction, Cl atoms were generated by the 266 nm photolysis of $(3-50) \times 10^{13}$ molecule cm^{-3} Cl_2SO. The 248 nm photolysis of Cl_2SO produces 76% of Cl($^2P_{3/2}$) and 24% of Cl*($^2P_{1/2}$).[46,47] Because Cl*($^2P_{1/2}$) atoms were rapidly relaxed to Cl($^2P_{3/2}$) by collisions with N_2 under our pressure conditions,[46] only Cl($^2P_{3/2}$) atoms reacted with DMS to give the Cl−DMS adduct that has a broad absorption band in the region from 270 to 450 nm.[18] In the present work, the Cl−DMS adduct was monitored using its absorption at 337−440 nm. Temporal changes in the concentration of the Cl−DMS adduct at 343 nm were used to determine the rate constant k_1.

All reagents were obtained from commercial sources, Wako Pure Chemicals. Cl_2SO (>95.0%) and DMS (98.0%) were subjected to repeated freeze−pump−thaw cycling before use. The dominant impurities in Cl_2SO were SO_2, HCl, and H_2SO_3, and in DMS it was CH_3SSCH_3. Research grade N_2 (>99.999%, Teisan) and O_2 (>99.995%, Teisan) were used without further purification.

3. Results and Discussion

Cl atoms were produced by the 266 nm photolysis of Cl_2SO at a total pressure of 20−300 Torr with N_2 diluent and T = 278−318 K in the presence of $(4-40) \times 10^{13}$ molecules cm^{-3} DMS. Figure 2 shows the rise and decay time profiles of the adduct Cl−DMS at different concentrations of DMS at 343 nm with 300 Torr of N_2 diluent. This absorption is attributable to the formation of Cl−DMS that absorbs in the region 270−450 nm. The CRDS absorption spectrum centered at each measured wavelength had no fine structures within our spectral resolution of <0.2 cm^{-1} . Referring to the absorption cross-section of Cl−DMS at 343 nm for a total pressure of 155 Torr with N_2 diluent reported by Urbanski et al.,[18] the absorption cross-sections of Cl−DMS at several wavelengths were determined in the present experiment (Table 2). The absorption cross-sections at 337 and 343 nm were corrected for the absorption of the reaction product, CH_3SCH_2, using the cross-section data of CH_3SCH_2 reported by Wallington et al.[48] Table 2 shows that our relative cross sections of Cl−DMS are in reasonable agreement with those reported by Urbanski et al.[18] Both the rise and decay rates increased with the DMS concentration. We checked the possibility of radical−radical reactions by changing the photolysis laser intensity for the range of 10−30 mJ. No laser power dependence was observed in the slopes of the rise and decay profiles. These results indicate no significant radical−radical reactions occurring. The pseudo-first-order rate constants for reaction 1 were determined from the double exponential fitting curves, which include the rise and decay profiles of Cl−DMS under excess concentration of DMS. The room-temperature rate constant of reaction 1 at 300 Torr N_2 diluents was determined to be $(4.2 \pm 0.4) \times 10^{-10}$ cm^3 molecule^{-1} s^{-1} from the second-order plots of reaction 1 shown in Figure 3

$$k_1' = k_1[\mathrm{DMS}] + k_d \quad (4)$$

where k_1' is the pseudo-first-order rate constant for reaction 1. Error bars are 1σ. k_d is the rate constant for diffusion and wall loss, which is obtained experimentally as the intercept at [DMS] = 0.

Pressure dependence of the rate constant of the reaction of Cl + DMS was measured for 20−300 Torr N_2 dilution. Those

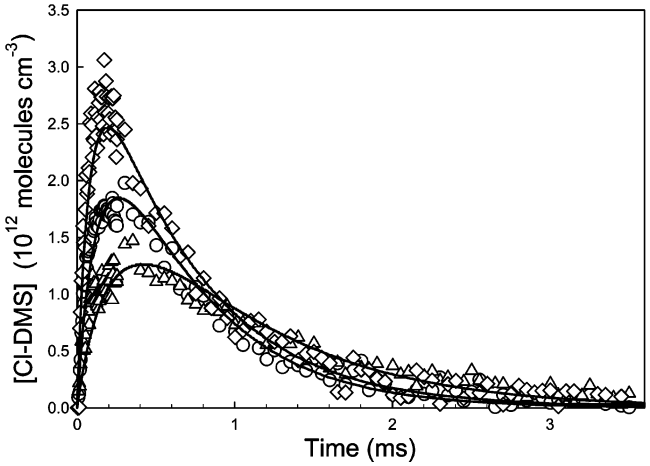

Figure 2. Time profiles of the Cl−S(CH$_3$)$_2$ adduct monitored at 343 nm at different concentrations of (CH$_3$)$_2$S: (◇) [(CH$_3$)$_2$S] = 2.8×10^{13} molecules cm^{-3}; (○) 1.6×10^{13} molecules cm^{-3}; (△) 8.1×10^{12} molecules cm^{-3}. Total pressure 300 Torr with N_2 diluent and T = 298 K. Solid curves are simulated ones. See the text for details.

TABLE 2: Absorption Cross-sections of the Cl−S(CH$_3$)$_2$ Adduct

	cross section (10^{-18} cm^2 molecule^{-1})	
wavelength (nm)	present work[a]	ref 18
337	36	32
343	29	33
400	11	9
440	1	2

[a] Error bars are 33% after reference 18 and error propagation.

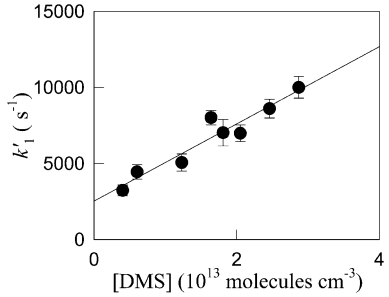

Figure 3. Second-order plots for the reaction of Cl atom with $(CH_3)_2S$ under 300 Torr of N_2 diluent at 298 K. The solid curve is a linear least-squares fit to eq 4.

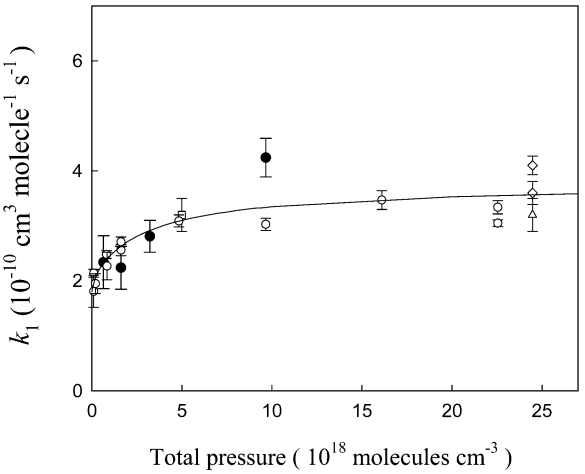

Figure 4. Rate constants of Cl atom with $(CH_3)_2S$ as a function of total pressure with N_2 diluent at 298 K. Fitting eq 5, the low- and high-pressure limit rate constants are determined to be $k_{1a}^{high} = (2.2 \pm 0.2) \times 10^{-10}$ cm^3 $molecule^{-1}$ s^{-1} and $k_{1a}^{low} = (2.2 \pm 0.7) \times 10^{-28}$ cm^6 $molecule^{-2}$ s^{-1}. $k_{1b} = 1.8 \times 10^{-10}$ cm^3 $molecule^{-1}$ s^{-1} [17] is used for intercept of this fitting curve. Key: present results (●); ref 17 (○); ref 18 (□); ref 49 (◇); ref 50 (△).

results are shown in Figure 4. The reaction of Cl + DMS includes two reaction channels. One reaction channel is the pressure dependent channel according to reaction 1a and the other is the pressure independent channel according to reaction 1b. Thus, as shown in Figure 4 the data are fit to Troe's expression (5) which includes the pressure independent term k_{1b} due to reaction 1b:

$$k_1 = k_{1b} + \left(\frac{k_{1a}^{low}[M]}{1 + (k_{1a}^{low}[M]/k_{1a}^{high})}\right) 0.6^{\{1+[\log(k_{1a}^{low}[M]/k_{1a}^{high})]^2\}^{-1}} \quad (5)$$

In this figure our data are combined with those by Stickel et al.,[17] Urbanski et al.,[18] Nielsen et al.,[49] and Kinnison et al.[50] Stickel et al. reported that (a) the HCl yield from reaction 1b approaches unity as the pressure approaches zero and (b) the rate constant k_{1b} is 1.8×10^{-10} cm^3 $molecule^{-1}$ s^{-1}. With k_{1b} fixed to the value reported by Stickel et al.,[17] the best-fit procedure provides the high-pressure limit rate constant of reaction 1a to be $k_{1a}^{high} = (2.2 \pm 0.2) \times 10^{-10}$ cm^3 $molecule^{-1}$ s^{-1} and the low-pressure limit of reaction 1a to be $k_1^{low} = (2.2 \pm 0.7) \times 10^{-28}$ cm^6 $molecule^{-2}$ s^{-1}. Thus, we estimate the rate constant of reaction 1 at atmospheric pressure to be k_1(760 Torr) $= (3.6 \pm 0.2) \times 10^{-10}$ cm^3 $molecule^{-1}$ s^{-1}. Stickel et al.[17] reported that (a) k_1 increased with pressure and (b) k_1(760 Torr) was $(3.3 \pm 0.5) \times 10^{-10}$ cm^3 $molecule^{-1}$ s^{-1}. Within the error bars, two experimental results are in agreement to each other.

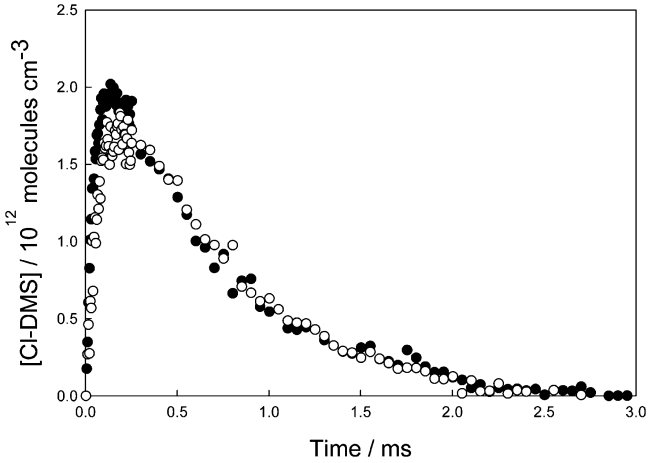

Figure 5. Time profiles of the $Cl-S(CH_3)_2$ adduct with O_2 (●) and without O_2 (○) under 100 Torr of N_2 diluent.

When 10 Torr of O_2 was added to the same experimental system, the time profile of Cl−DMS was the same as shown in Figure 5. These results indicate that the reaction of Cl−DMS with O_2 is so slow that it does not compete with other reactions.

Using our theoretically calculated K value for Cl−DMS and the experimentally obtained forward rate constant k_{1a} for 300 Torr, the rate constant of the backward reaction (−1a) is determined to be 90 ± 20 s^{-1}. To check our kinetic models with the IBM Kinetics Simulator, we simulated the rise and decay curves for $[DMS]_0 = (0.8-2.8) \times 10^{13}$ molecules cm^{-3}, $k_{1a} = 2.4 \times 10^{-10}$ $cm^3 molecule^{-1}$ s^{-1}, $k_{-1a} = 90$ s^{-1}, and $k_{1b} = 1.8 \times 10^{-10}$ cm^3 $molecule^{-1}$ s^{-1} [17] with the parameters $[Cl]_0 = (4.0-5.5) \times 10^{12}$ cm^3 $molecule^{-1}$ s^{-1} and $k_d = 1500-2000$ s^{-1}. The fitting curves are shown by the solid curves in Figure 2 for the three different concentrations of DMS. The simulated rise and decay curves are in agreement with the data, confirming that (a) our kinetic model is appropriate and (b) the obtained rate constants and the equilibrium constant are reasonable. However, k_{-1a} is much smaller than the adjustment range of k_d in the simulation procedure. In addition, the simulation fitting depends on $[Cl]_0$. Hence, it is safe to say that the rate constant k_{-1a} is about a few hundred in a unit of s^{-1}.

The reactions of Cl with DMS proceed via two reaction channels;

$$Cl + CH_3SCH_3 + M \rightleftarrows Cl-DMS + M \quad (1a, -1a)$$

$$Cl + CH_3SCH_3 \rightarrow HCl + CH_3SCH_2 \quad (1b)$$

The reactions of Br with DMS also proceed via the forward reaction channels and back-reaction (−6a):

$$Br + CH_3SCH_3 + M \rightleftarrows Br-DMS + M \quad (6a, -6a)$$

$$Br + CH_3SCH_3 \rightarrow HBr + CH_3SCH_2 \quad (6b)$$

The rapid unimolecular decomposition rate $k_{-6a} = (1.02 \pm 0.07) \times 10^4$ s^{-1} of the Br−DMS adduct reflects the weakness of the Br−S bond determined experimentally (12 ± 1 kcal mol^{-1}).[14] On the basis of the present calculated results and previously reported values, the heat of formation of Cl−DMS (ΔH_f° = −12 to −19 kcal mol^{-1}) is not so different from that of Br−DMS. Hence, the present rate constant of the backward reaction k_{-1a} of a few hundred s^{-1} is reasonable.

4. Atmospheric Implications

The rapid decay of Cl−DMS within a few milliseconds was observed in Figure 2. Thus, the only atmospheric species capable

of scavenging the Cl−DMS adduct on a time scale competitive with reaction (−1a) would be O_2:

$$\text{Cl−DMS} + O_2 \rightarrow \text{DMSO} + \text{ClO} \qquad (7)$$

An upper limit value of $k_7 < 4 \times 10^{-18}$ cm^3 molecule^{-1} s^{-1} was reported by Stickel et al.[17] for the reaction of the Cl−DMS adduct with O_2. Under the condition of 1 atm of the air, the lifetime of Cl−DMS with respect to the reaction with O_2 is >0.05 s. Thus, we conclude that the atmospheric fate of Cl−DMS is not the direct reaction with O_2, but the thermal decomposition via reaction (−1a).

On the basis of our recent results for the reaction of DMS with Br, the Br−DMS adduct essentially has no importance in atmospheric chemistry because of its rapid back-reaction, whereas the reactions with IO or BrO are important oxidation reactions for DMS.[14,15] Thus, the X−DMS adducts for X = Cl or Br are not an important sink of DMS in the atmosphere.

Acknowledgment. We thank S. Nakamichi, J. Ueda, and M. Goto for their help with the experiment and analysis. This work is supported in part by a Grants-in-Aid from the Ministry of Education, Japan, in the priority research field "Radical Chain Reactions".

Supporting Information Available: Table of calculated harmonic virbational frequencies, rotational constants, and optimized geometries. This material is available free of charge via the Internet at http://pubs.acs.org.

References and Notes

(1) Cullis, C. F.; Hirschler, M. M. *Atmos. Environ*. **1980**, *14*, 1263.
(2) Andreae, M. O.; Ferek, R. J.; Bermond, F.; Byrd, K. P.; Engstrom, R. T.; Hardin, S.; Houmere, P. D.; Le Marrec, F.; Raemdonck, H.; Chatfield, R. B. *J. Geophys. Res*. **1985**, *90*, 12891.
(3) Bates, T. S.; Lamb, B. K.; Guenther, A.; Dignon, J.; Stoiber, R. E. *J. Atmos. Chem*. **1992**, *14*, 315.
(4) Kettle, A. J.; Andreae, M. O. *J. Geophys. Res*. **2000**, *105*, 2679.
(5) Shon, Z. H.; Davis, D.; Chen, G.; Grodzinsky, G.; Bandy, A.; Thornton, D.; Sandholm, S. Bradshaw, J.; Stickel, R.; Chameides, W.; Kok, G.; Russell, L.; Mauldin, L.; Tanner, D.; Eisele, F. *Atmos. Environ*. **2001**, *35*, 159.
(6) Tyndall, G. S.; Ravishankara, A. R. *Int. J. Chem. Kinet.* **1991**, *23*, 483.
(7) Sekušak, S.; Piecuch, P.; Bartlett, R. J.; Cory, M. G. *J. Phys. Chem. A* **2000**, *104*, 8779.
(8) Cooper, D. J. *J. Atoms. Chem*. **1996**, *25*, 97.
(9) Ravishankara, A. R.; Rudich, Y.; Talukdar, R.; Barone, S. B. *Philos. Trans. R. Res. London. Ser. B* **1997**, *352*, 171.
(10) Allan, B. J.; McFiggans, G.; Plane, J. M. C.; Coe, H.; McFadyen, G. G. *J. Geophys. Res*. **2000**, *105*, 24191.
(11) Charlson, R. J.; Lovelock, J. E.; Andreae, M. O.; Warren, S. G. *Nature* **1987**, *326*, 655.
(12) McFiggans, G.; Cox, R. A.; Mossinger, J. C.; Allan, B. J.; Plane, J. M. C. *J. Geophys. Res.* **2002**, *107*, 15.
(13) Barnes, I.; Becker, K. H.; Overath, R. D. *Tropospheric Chemistry of Ozone in the Polar Regions*; Niki, H., Becker, K. H., Eds.; ; NATO ASI Series 1, Global Environmental Change; Springer: Berlin, 1993; 1 7, p 371.
(14) Nakano, Y.; Goto, M.; Hashimoto, S.; Kawasaki, M.; Wallington, T. J. *J. Phys. Chem. A* **2001**, *105*, 11045.
(15) Nakano, Y.; Enami, S.; Nakamichi, S.; Aloisio, S.; Hashimoto, S.; Kawasaki, M. *J. Phys. Chem. A* **2003**, *107*, 6381.
(16) Finlayson-Pitts, B. J.; Pitts, J. N. *Chemistry of the Upper and Lower Atmosphere: Theory, Experiments and Applications*; Academic Press: San Diego, CA, 2000.
(17) Stickel, R. E.; Nicovich, J. M.; Wang, S.; Zhao, Z.; Wine, P. H. *J. Phys. Chem*. **1992**, *96*, 9875.
(18) Urbanski, S. P.; Wine, P. H. *J. Phys. Chem. A* **1999**, *103*, 10935.
(19) O'Keefe, A.; Deacon, D. D. G. *Rev. Sci. Instrum.* **1988**, *59*, 2544.
(20) Zalicki, P.; Zare, R. N. *J.* Chem. Phys. **1995**, *102*, 2708.
(21) Berden, G.; Peeters, R.; Meijer, G. *Int. Rev. Phys. Chem*. **2000**, *19*, 565.
(22) King, M. D.; Dick, E. M.; Simpson, W. R. *Atmos. Environ*. **2000**, *34*, 685.
(23) Tonokura, K.; Marui, S.; Koshi, M. *Chem. Phys. Lett*. **1999**, *313*, 771.
(24) Yu, T.; Lin M. C. *J. Am. Chem. Soc*. **1993**, *115*, 4371.
(25) Yu, T.; Lin M. C. *J. Am. Chem. Soc*. **1994**, *116*, 9571.
(26) Yu, T.; Lin M. C. *J. Phys. Chem.* **1994**, *98*, 9697.
(27) Yu, T.; Lin M. C. *J. Phys. Chem.* **1995**, *99*, 8599.
(28) Yu, T.; Lin M. C. *Int. J. Chem. Kinet.* **1993**, *25*, 875.
(29) Yu, T.; Lin M. C. *Int. J. Chem. Kinet.* **1994**, *26*, 771.
(30) Lin M. C. *J. Phys. Chem.* **1994**, *98*, 2105.
(31) Atkinson D. B.; Hundgens J. W. *J. Phys. Chem. A* **1997**, *101*, 3901.
(32) Wheeler, N. D.; Newman, S. M.; Orr-Ewing, A. J.; Ashfold, M. N. R. *J. Chem. Soc., Faraday Trans*. **1998**, *94*, 337.
(33) Yu, T.; Lin, M. C. *J. Phys. Chem*. **1994**, *98*, 9697.
(34) Zhu, L.; Johnston, G. *J. Phys. Chem*. **1995**, *99*, 15114.
(35) Atkinson, D. B.; Hudgens, J. W. J. W.; Orr-Ewing, A. J. *J. Phys. Chem. A* **1999**, *103*, 6173.
(36) Brown, S. S.; Wilson, R. W.; Ravishankara, A. R. *J. Phys. Chem. A* **2000**, *104*, 4976.
(37) Brown, S. S.; Ravishankara, A. R.; Stark, H. *J. Phys. Chem. A* **2000**, *104*, 7044.
(38) Frisch, M. J.; Trucks, G. W.; Schlegel, H. B.; Scuseria, G. E.; Robb, M. A.; Cheeseman, J. R.; Zakrzewski, V. G.; Montgomery, J. A.; Stratmann, R. E.; Burant, J. C.; Dapprich, S.; Millam, J. M.; Daniels, A. D.; Kudin, K. N.; Strain, M. C.; Farkas, O.; Tomasi, J.; Barone, V.; Cossi, M.; Cammi, R.; Mennucci, B.; Pomelli, C.; Adamo, C.; Clifford, S.; Ochterski, J.; Petersson, G. A.; Ayala, P. Y.; Cui, Q.; Morokuma, K.; Malick, D. K.; Rabuck, A. D.; Raghavachari, K.; Foresman, J. B.; Cioslowski, J.; Ortiz, J. V.; Stefanov, B. B.; Liu, G.; Liashenko, A.; Piskorz, P.; Komaromi, I.; Gomperts, R.; Martin, R. L.; Fox, D. J.; Keith, T.; Al-Laham, M. A.; Peng, C. Y.; Nanayakkara, A.; Gonzalez, C.; Challacombe, M.; Gill, P. M. W.; Johnson, B. G.; Chen, W.; Wong, M. W.; Andres, J. L.; Head-Gordon, M.; Replogle E. S.; Pople, J. A. *Gaussian 98*, revision A.7; Gaussian, Inc.: Pittsburgh, PA, 1998.
(39) McKee, M. L. *J. Phys. Chem.* **1993**, *97*, 10971.
(40) Resende, S. M.; De Almeida, W. B. *J. Phys. Chem. A* **1997**, *101*, 9738.
(41) Wilson, C.; Hirst, D. M. *J. Chem. Soc., Faraday Trans*. **1997**, *93*, 2831.
(42) McQuarrie, D. A. *Statistical Mechanics*; University Science Books: Sausalito CA, 2000.
(43) Levchenko, S. V.; Krylov, A. L. *J. Phys. Chem A* **2002**, *106*, 5169.
(44) Ninomiya, Y.; Hashimoto, S.; Kawasaki, M.; Wallington, T. J. *Int. J. Chem. Kinet*. **2000**, *32*, 125.
(45) Brown, S. S.; Ravishankara, A. R.; Stark, H. *J. Phys. Chem*. **2000**, *104*, 7044.
(46) Kawasaki, M.; Suto, K.; Sato, Y.; Mastumi, Y.; Bersohn, R. *J. Phys. Chem*. **1996**, *100*, 19853.
(47) Sotnichenko, S. A.; Bokun, V. C.; Nadkhin, A. I. *Chem. Phys. Lett*. **1988**, *153*, 560.
(48) Wallington, T. J.; Ellermann, T.; Nielsen, O. J. *J. Phys. Chem*. **1993**, *97*, 8442.
(49) Nielsen, O. J.; Sidebottom, H. W.; Nelson, L.; Rattigan, O.; Treacy, J. J.; O'Farrell, D. J. *Int. J. Chem. Kinet.* **1990**, *22*, 603.
(50) Kinnison, D. J.; Mengon, W.; Kerr, J. A. *J. Chem. Soc., Faraday Trans.* **1996**, *92*, 369.